# REPORT DOCUMENTATION PAGE

*Form Approved*
*OMB No. 0704-0188*



| 1. REPORT DATE *(DD-MM-YYYY)* | 2. REPORT TYPE | 3. DATES COVERED *(From - To)* |
|---|---|---|
| 15-10-1996 | Final Report | to 15-9- 1996 |

**4. TITLE AND SUBTITLE**
Magnetic Shielding for High Fields
Final Report

Volume : ()

**5a. CONTRACT NUMBER**
DAAE30-96-C-0023

**5b. GRANT NUMBER**

**5c. PROGRAM ELEMENT NUMBER**

**6. AUTHOR(S)**
Biter, William J; Author

**5d. PROJECT NUMBER**

**5e. TASK NUMBER**

**5f. WORK UNIT NUMBER**

**7. PERFORMING ORGANIZATION NAME(S) AND ADDRESS(ES)**

Sensortex, Inc.
515 Schoolhouse Road
Kennett Square, PA 19348

**8. PERFORMING ORGANIZATION REPORT NUMBER**
C105F

**9. SPONSORING / MONITORING AGENCY NAME(S) AND ADDRESS(ES)**
Department of the Army
US Army ARDEC
Piscataway, NJ 07806

**10. SPONSOR/MONITOR'S ACRONYM(S)**
ARDEC

**11. SPONSOR/MONITOR'S REPORT NUMBER(S)**
0001AB

**12. DISTRIBUTION / AVAILABILITY STATEMENT**
A Approved for public release; distribution is unlimited.

**13. SUPPLEMENTARY NOTES**
The findings contained in this report are those of the author and should not be contrued as an official Army position, policy, or decision, unless designated by other documentation.

**14. ABSTRACT**
During the program a code was developed to predict the attenuation in a multilayer, non-linear system. This program allows modeling of shielding effectiveness for the complex case of high conductivity and high permeability layers in which the high permeability film reaches saturation. Conventional materials have limited effectiveness once they saturated but, using this code, it is possible to design a profile to increase the attenuation even at magnetic fields that saturate the magnetic layers. This is a surprising result and indicates the importance of a code that treats nonlinear, multilayer media.

**15. SUBJECT TERMS**
shielding; magnetic; EMP; rail guns; conductors; thin films; multilayers

| 16. SECURITY CLASSIFICATION OF: | | | 17. LIMITATION OF ABSTRACT | 18. NUMBER OF PAGES | 19a. NAME OF RESPONSIBLE PERSON |
|---|---|---|---|---|---|
| a. REPORT | b. ABSTRACT | c. THIS PAGE | Unclassified Unlimited | 25 | William Biter |
| UNCLASSIFIED | UNCLASSIFIED | UNCLASSIFIED | | | 19b. TELEPHONE NUMBER *(include area code)* 610-444-2383 |

**Sensortex, Inc.**
**P.O. Box 644**
**Unionville, PA 19375-0644**
**(610)444-2383**
**October 15, 1996**

# Magnetic Shielding for High Fields

**Contract # DAAE30-96-C-0023**

## Final Report

# Form SF298 Citation Data

| **Report Date** *("DD MON YYYY")* 15101996 | **Report Type** Final | **Dates Covered (from... to)** *("DD MON YYYY")* 15091996 |
|---|---|---|

| | |
|---|---|
| **Title and Subtitle** Magnetic Shielding for High Fields | **Contract or Grant Number** DAAE30-96-C-0023 |
| | **Program Element Number** |
| **Authors** Biter, William J | **Project Number** |
| | **Task Number** |
| | **Work Unit Number** |
| **Performing Organization Name(s) and Address(es)** Sensortex, Inc. 515 Schoolhouse Road Kennett Square, PA 19348 | **Performing Organization Number(s)** C105F |
| **Sponsoring/Monitoring Agency Name(s) and Address(es)** Department of the Army US Army ARDEC Piscataway, NJ 07806 | **Monitoring Agency Acronym** ARDEC |
| | **Monitoring Agency Report Number(s)** 0001AB |

**Distribution/Availability Statement**
Approved for public release, distribution unlimited

**Supplementary Notes**
The findings contained in this report are those of the author and should not be construed as an official Army position, policy, or decision, unless designated by other documentation.

**Abstract**
During the program a code was developed to predict the attenuation in a multilayer, non-linear system. This program allows modeling of shielding effectiveness for the complex case of high conductivity and high permeability layers in which the high permeability film reaches saturation. Conventional materials have limited effectiveness once they saturated but, using this code, it is possible to design a profile to increase the attenuation even at magnetic fields that saturate the magnetic layers. This is a surprising result and indicates the importance of a code that treats nonlinear, multilayer media.

**Subject Terms**
shielding; magnetic; EMP; rail guns; conductors; thin films; multilayers

| **Document Classification** unclassified | **Classification of SF298** unclassified |
|---|---|

| | |
|---|---|
| **Classification of Abstract**<br>unclassified | **Limitation of Abstract**<br>unlimited |
| **Number of Pages**<br>25 | |

# Table Of Contents

## 1.0. Summary

During the program a code was developed to predict the attenuation in a multilayer, non-linear system. This program allows modeling of shielding effectiveness for the complex case of high conductivity and high permeability layers in which the high permeability film reaches saturation. Conventional materials have limited effectiveness once they saturated but, using this code, it is possible to design a profile to increase the attenuation even at magnetic fields that saturate the magnetic layers. This is a surprising result and indicates the importance of a code that treats nonlinear, multilayer media.

Finding a mathematical solution in the Phase I also changed the direction of the proposed Phase II program. Originally, the program was to be aimed at producing and marketing a new shielding material. This continues to be a longer range goal but the initial Phase II will be directed to market a user-friendly version of the code developed during the phase I program. This will be followed by development of the profiled shielding material for high magnetic fields. This requires a higher levels of capital investment for both production and marketing and will be delayed until the code has been marketed.

During the phase I program, multilayer films consisted of alternating layers of permalloy copper were also fabricated and measured. However, the results for the model and the design of the profile, were obtained too late in the program to be experimentally verified.

## 2.0. Code Development

Nonlinearity produces switching causing decomposition of the original signal into time harmonic components leading to inherent insertion loss at the frequency of interest (the frequency multiplication relying on the steepness of the B-H curve). Based on preliminary but sound time domain FDTD (Finite Difference Time Domain) extensive numerical simulations we have demonstrated the feasibility of a novel wide bandwidth shielding material. Preliminary up-optimized data reveals significant shielding advantages (9.5 dB) with respect to a sigma-mu layered configuration prevalent in modern low frequency shielding materials. The new composite material being nonlinear magnetic and layered has a suitable profile in its saturation characteristics. We speculate that the observed transmitted field is a solid like solution. Correspondingly we propose to establish in Phase II the theoretical foundation of the new composite and ascertain that the new material can be produced having the desired shielding capacity, while being lightweight, flexible, and cost effective. In the process of this investigation, Sensortex, Inc. has developed a design tool. This tool is a normal incidence layered version of a nonlinear FDTD code that is expected to be enhanced in Phase II with a variety of capabilities and user friendly items in order to define a commercial product.

## 3.0. Shielding Background

Shielding of electromagnetic radiation has been extensively studied in the engineering literature and the problems are well identified. The problems are generally connected with the available materials and involve tradeoffs between weight, cost and SE (shielding efficiency).

Rail guns have additional problems. Fields generated by these guns are low frequencies, low impedance high intensity near-field waves, with intensities from 1 to 10 Telasa, which will saturate most shields. In addition, the efficiency of the gun itself can be degraded by interaction with the magnetic shielding if they are too massive or too close.

For low impedance waves (near field, magnetic), the front surface reflection can be considerably less and the attenuation after the wave has entered the metal is the dominant loss mechanism. This attenuation is usually maximized by using a metal with a high μ since this gives the smallest penetration depths. Typically, shielding relying on absorption ends with thick magnetic panels, which drastically increases the weight, cost and complexity of a structure.

There is a further complication when relying on magnetic films. Such films obtain the high attenuation by a small skin depth, given by:

$$\delta = \frac{1}{\sqrt{\pi \mu \sigma f}} \ (meters) \tag{1}$$

where σ is the conductivity, f is the frequency and μ the permeability. Magnetic materials have permeabilities over 100,000 so the skin depth is very small. But since saturated flux density are normally below 2 T, this also means that high permeability films saturate at a low level of field.

The initial approach for the Phase I program was the use of layered films, consisting of laminar composites of the good conductor and a high μ.. Such films achieve good SE for both plane waves and magnetic waves. When the thickness of the individual layer are smaller than the penetration depth, the electrical and magnetic properties are effectively averaged and the DE is increased by and increase in the σμ product, not simply by increasing μ.

These materials are attractive since, for the same thickness of the magnetic film, they have increased performance so that a lightweight structure can be made with good shielding at low frequencies. An additional feature is superior performance at high fields that would saturate most magnetic shields. These films obtain increased performance from the higher average conductivity and the lower average μ. The best performance in a high field environment will occur with multilayer structures with a high percentage of the conductor. This also means the films will be low cost (copper is cheaper than nickel) and have minimal interference with the rail gun ($\mu_{ave}$ * thickness is low).

### 3.1. Saturation

Saturation is determined by the composition and crystal lattice structure of the material. This saturation is basically the complete alignment of all the domains in the material. At higher field the magnetization will continue to increase but very slowly. This is due to the spontaneous magnetization within a single domain and is known as forced magnetization.

Cobalt-iron alloys have some of the highest saturation values, with ~ 35% cobalt saturating at 2.43 T. Pure iron is also very high while the various silicon alloys of iron saturate near 2.0 T. The nickel/iron alloys (permalloys) range up to 1.6 T (50/50). Saturation fields of some common material are given in Table I.

Table I

| Material | Saturation Flux (Telsas) |
|---|---|
| Iron | 1.71 |
| Cobalt | 1.42 |
| Permalloy 50/50 | 1.6 |
| Permalloy78/22 | 0.86 |
| Metglas | 1.27 |
| 50/50 Co/Fe | 1.91 |
| 37/65 Co/FE | 2.35 |
| Nickel | 0.6 |

This is a very basic and fundamental problem with magnetic shielding. Good shielding against magnetic fields normally requires high permeability material. Since the saturation values occur between 1 and 2 Telsas and since $B = \mu H$, a high $\mu$ material will saturate at low external fields. The exception to this occurs with the multilayer films where multiple internal reflections and high conductivity account for a significant amount of the magnetic shielding. Additional results from the Phase I program also indicates that, with the proper profile, the shielding can actually increase once the magnetic film saturates.

### 3.2. Multi-Layers Shielding

A standard technique in shielding construction is to use two layers of shielding separated by an air gap [1]. It increases the SE from an additional reflection at the second material and also reduces the field in the second layer, which minimizes saturation problems. The multilayer material, Thinshield, has improved shielding both from an averaging of the constituent material and increased reflection occurring at each of the multiple interfaces.

The material, Thinshield [4,5,6], has additional shielding by an interaction between the composite materials as a result of the mixing of the electrical properties. The interaction of the EM field depends on the interaction between the layers. An increase in absorption compared to simple stacking the films was predicted from the concept of effective media, where the layering averages the electrical properties of the two films.

In the effective media approximation, a layered structure with the layers thin compared to changes in the fields within a layer, the properties of the total structure can be treated as a volume average of the electrical properties of the separate media. With very thin laminar films, this reduces to simple thickness averages of the susceptibility and the conductivity. For high $\mu$ materials, this can be approximated by

$$\mu_{ave} \sim \frac{\mu_1 t_1 + \mu_2 t_2}{t_1 + t_2}, \tag{2}$$

where $\mu_{1,2}$ and $t_{1,2}$ refer to the permeability and thickness of the respective layers. Similarly, the average conductivity is given by

$$\sigma_{ave} = \frac{\sigma_1 t_1 + \sigma_2 t_2}{t_1 + t_2}. \tag{3}$$

If $\sigma$ of the magnetic film is much less than that of the conductive film, and $\mu$ of the conductive film is much less than that of the magnetic film, then the averaging of the conductivity and permeability increases their $\mu\sigma$ product, which decreases the skin depth, or:

$$\mu_{ave}\sigma_{ave} > \mu_{mag}\sigma_{mag} > \mu_{cond}\sigma_{cond}. \quad (4)$$

These conditions are true for most highly magnetic films and predict that the layered material will have a higher absorption than either material treated separately.

The effective media approximation is an intuitively simple method of looking at the detailed interaction occurring within a layered structure. There are various programs that solve (exactly) the wave equation in a multi-layered material. Using these programs, the individual layers, with their respective $\sigma$ 's and $\mu$'s are used, not the average properties. The effective media concept simply allows insight into the mechanisms by replacing the multilayer solution with the simple equation for attenuation (eq. 4):

$$E=E_o e^{(-z/\delta)} \quad (5)$$

where $\delta$ is the average $\delta$ using $\sigma_{ave}$ and $\mu_{ave}$ and z is the total film thickness. This allows us to predict very simply that the attenuation from the averaged film is much higher than simply stacking the same two materials (this is the case when the thickness of each layer is large).

### 3.3. High Field Performance

Although the code developed during the phase I program can treat the saturated films, a simple approximation indicated the potential improvement before saturation. The averaging of the multilayers increase the absorption by increasing the $\sigma\mu$ product. This occurs from a significant increase in $\sigma_{ave}$, which is also accompanied by a decrease in $\mu_{ave}$. For most films the maximum value of $\sigma\mu$ occurs near 50/50, however this value decreases only slightly with changes in composition. In particular, increasing the percentage of the high $\sigma$ material decreases the $\sigma\mu$ product slightly but has a significant effect on the average value of the $\mu$. Assuming $B_{sat}= \mu_{ave}H_{sat}$, a decreased $\mu_{ave}$ will increase the value for $H_{sat}$ at a given $B_{max}$. This means the field required for saturation has increased even though the absorption still remains high.

Figure 1 plots the values for $H_{sat}$ versus the percentage copper based on a copper/permalloy stack. A saturation value of 1.6 T (50/50 permalloy) was used for the permalloy. At a 90/10 ratio of copper/permalloy, the material does not saturate until an external field of 160 Oe, twice the saturation field for iron. Thickness required to give a 20 dB absorption at 10 kHz versus the percentage copper is shown in Figure 1. This film still has an 20 dB absorption at a thickness of 6 mils (.006").

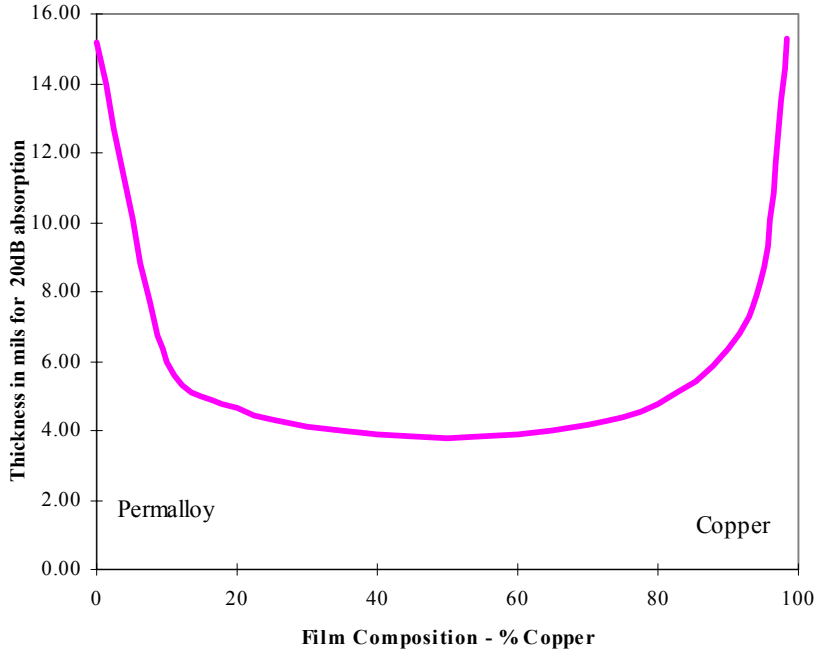


Figure 1. Calculated thickness to produce 20 dB absorption vs. mixing ratio.

## 4.0. The Analytical Problem

The geometry of interest consists of a multi-layered configuration each consisting of a lossy dielectric and nonlinear magnetic material. The characteristic layer parameters are a dielectric constant, a conductivity, and low signal permeability coupled with magnetic saturation levels. The illumination is assumed to be a plane wave normally incident on the layered structure. Our interest is in the calculation of the reflected and transmitted fields. Figure 2 depicts the stratified problem.

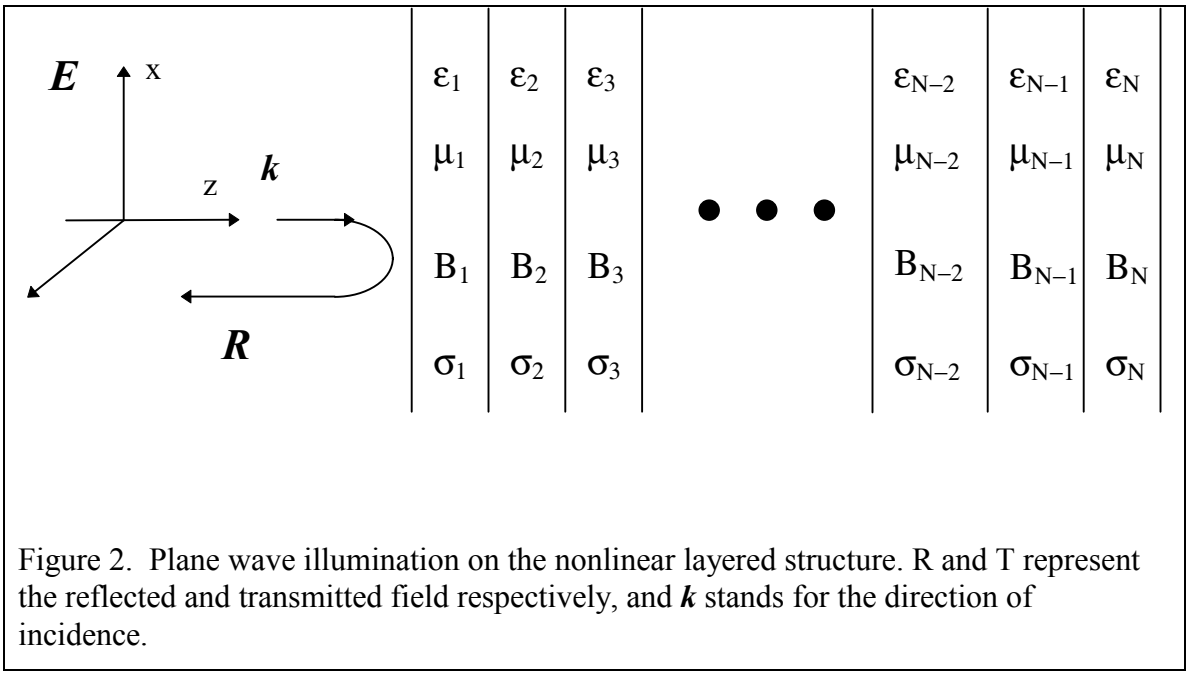


Figure 2. Plane wave illumination on the nonlinear layered structure. R and T represent the reflected and transmitted field respectively, and ***k*** stands for the direction of incidence.

Due to the nonlinear nature of the problem, the analysis can be performed either: (a) approximately, via a power expansion in harmonics, which is both elaborate and tedious, and most importantly, not very appropriate in view of the high nonlinearity (large changes in permeability), and (b) exactly, via a time domain scheme.

Evidently, the proper scheme for us is to pursue the solution in the time domain. Superposition is not applicable, therefore the source must be assumed to be sinusoidal.

A solution in the form of a set of integral equations is possible, however not of easy implementation, awkward, and possibly plagued by numerical difficulties (of the type encountered in the Sommerfeld/Brillouin precursors). A more robust numerical scheme is afforded by the direct solution of the field equations in differential form, which also has a past history of flexibility in modeling inhomogeneities, and successful in the treatment of certain kind of dispersive effects. This is the preferred scheme, and is detailed in the next section.

### 4.1. The Finite Difference Time Domain Scheme(FDTD)

This is a conceptually simple, yet powerful technique for obtaining solutions to electromagnetic propagation problems. It is based on the gridding of the propagation space to a resolution fine enough to represent the field fluctuations (typically of the order of 10 cells per wavelength in the material for the lossless case), followed by application of the differential field equation operators (curl) in a finite difference sense, with a corresponding temporal step size.

The procedure is repeated sequentially, allowing the resulting code to run until the solution attains periodic "steady state" behavior. Under ideal conditions the numerical model would extend to infinity; computer limitations, however limit the amount of cells that can be handled. It is then necessary to perform a truncation of the numerical space. During this process it is important to ensure that the reflected and transmitted fields propagate freely off the finite grid so that spurious scattering off the edge regions do not contaminate the results. This necessitates the introduction of special conditions at the edges, the so called "absorbing boundary conditions". The method appears specially suited to the kind of magnetic nonlinearities we now encounter.

The field equations are of the form:

$$\nabla \times \overline{E} = -\frac{\partial \overline{B}}{\partial t} \tag{6}$$

$$\nabla \times \overline{H} = \varepsilon(z)\frac{\partial \overline{E}}{\partial t} + \sigma(z)\,\overline{E} \tag{7}$$

$$\overline{B} = \mu(\overline{H})\,\overline{H} \tag{8}$$

which for the layered case reduce to the scalar differential equations

$$\frac{\partial E}{\partial z} = -\frac{\partial B}{\partial t} \tag{9}$$

$$\frac{\partial H}{\partial z} = -\varepsilon(z)\,\frac{\partial E}{\partial t} - \sigma(z)\,E \tag{10}$$

$$B = \mu(H)\,H \tag{11}$$

where the field variables E, H and B are functions of z and t. The material parameters are unconstrained functions of z, and in particular the magnetic nonlinearity will be specified via the z dependent parameters:

v: a measure of the sharpness of the hysterisis curve
bco: the normalized saturation value of B
mu: the small signal (normalized) permeability.

Under deep saturation μ becomes 1, and it is assumed at this stage that the magnetic material is lossless, i.e., there is no area under the H-B curve. Figure 3 illustrates the H-B dependence (in normalized h and b respectively) for selected parameter values.

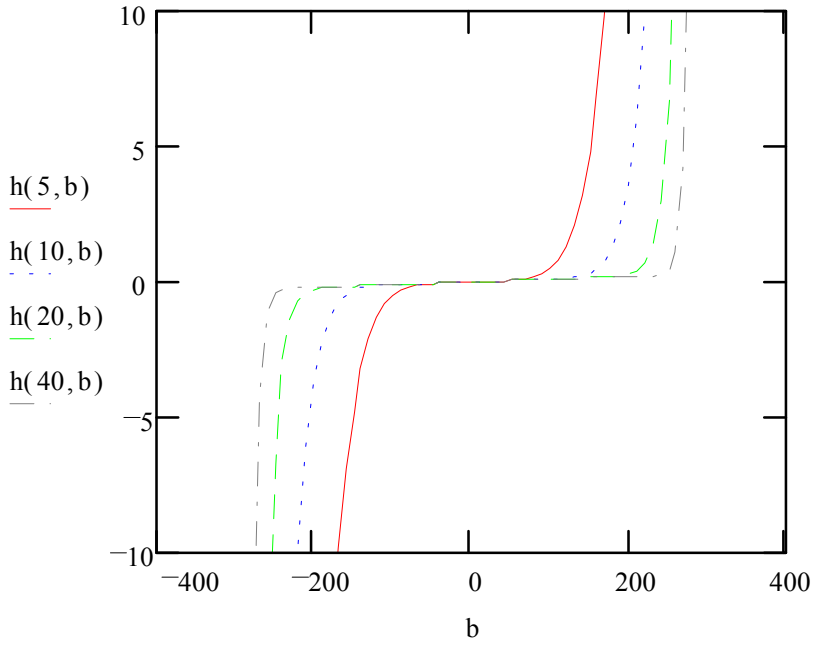


Figure 3. Normalized h-b nonlinear dependence for our simplified lossless model with bco=300, mu=1000, and v in the range 5 to 40.

To simplify the presentation, the discretization is done according to the following notation:

$$(z_i, t_j) \rightarrow (i, j) \qquad (12)$$

where $t_j$ denotes the jth discrete time, whereas $z_i$ refers to the centroid of the ith layer. The number of layers is N, however, we have found that successful implementation of the scheme can be achieved by truncating the model in the very neighborhood of the physical boundaries. This actually results in a total of N+6 numerical layers, since we introduce three artificial free space layers at each end of the structure for the purpose of graceful termination of the numerical model and implementation of the "reflectionless" boundaries via numerical enforcement of absorbing conditions.

Thus, the first three and the last three numerical layers are free space. All layers are taken to be of identical thickness δz, and the time step is equal to δt. This results in some simplification in the implementation. This is detailed next.

### 4.2. Reflection Region

In the free space region the scattered field components are related via:

$$H^s = -\frac{E^s}{\eta_0} \tag{13}$$

where each is a function of the form $f(z + c_0 t)$. Here $c_0$ and $\eta_0$ correspond to speed of light and impedance in free space. In view of this, Taylor expansion of the scattered electric field in (z,t) at point (n+1,m) results in:

$$E^s(n, m+1) = E^s(n+1, m) + (c_0 \delta t - \delta z) \left.\frac{\partial E^s}{\partial z}\right|_{(n+1,m)} . \tag{14}$$

In order to retain accuracy to second order, it is necessary to employ central differences (over a length 2 $\delta z$) for the above derivative. This results in

$$E^s(n, m+1) = E^s(n+1, m) + \frac{\nu}{2}\left(E^s(n+2, m) - E^s(n, m)\right), \tag{15}$$

where

$$\nu = \frac{c_0}{\beta} - 1 \quad , \quad \beta = \frac{\delta z}{\delta t} \tag{16}$$

for $\beta$ playing the role of a numerical speed, which must be larger or equal to $c_0$ for stability of the numerical scheme. Equation (15) is not applicable to the incident field since the direction of propagation is opposite to that of the reflected field. The difference is however minor as it translates in a change of sign in the parenthesis of (14). Addition of the incident field to (15) and after some manipulations, reduces to a recurrence expression for the total electric field on the reflected free space side:

$$E(n, m+1) = E(n+1, m) + \frac{\nu}{2}\left(E(n+2, m) - E(n, m)\right) + \Psi \tag{17}$$

$$\Psi = E^{inc}(n, m+1) - E^{inc}(n+1, m-1) - E^{inc}(n, m) + E^{inc}(n+1, m) \tag{18}$$

for $\Psi$ having the effect of a forcing function.

The total H field is composed of the incident plus scattered H fields. The incident fields are related in a fashion similar to (13), except that with a plus sign. As the scattered E field is total minus incident, the total magnetic field in the free space reflection region is given by:

$$B = \frac{1}{c_0}\left(2E^{inc} - E\right) . \qquad (19)$$

### 4.3. Transmission Region

On the transmitted side (three free space artificial layers) the total fields are related via

$$H = \frac{E}{\eta_0} , \qquad (20)$$

each of which is of the form $f(z - c_0 t)$. The analysis proceeds as previously, and the following differential form is obtained for the transmitted electric field:

$$E(n+1, m+1) = E(n, m) - \frac{\nu}{2}\left(E(n+1, m) - E(n-1, m)\right) . \qquad (21)$$

The corresponding magnetic field being given by

$$B = \frac{E}{c_0} . \qquad (22)$$

It should be noted that care is exercised (via analytical subtleties) in obtaining a second order accurate relation which allows proper time stepping.

### 4.4. Material Region

This region is particularly delicate in view of the fact that the conductivity of the layers may be very high, leading to numerical difficulties and inaccuracies. After some extensive testing we found out that the proper perfect conductivity can be achieved via the algorithm which is presented next.

The discretization of (10) results in

$$E(n, m+1) = E(n, m-1) - 2\delta t \frac{\sigma(n)}{\varepsilon(n)} E(n, m) - \frac{1}{\beta \varepsilon(n)}\left(H(n+1, m) - H(n-1, m)\right) . \qquad (23)$$

It can be shown after some iterations that in the limit of perfect conductivity this equation leads to an incorrect time stepping scheme. The subtle point is to replace the E(n,m) term by its central time average: [E(n,m+1)+E(n,m-1)]/2. After some rearrangement the above becomes:

$$E(n, m+1) = \left\{\frac{1 - \sigma(n)\delta t / \varepsilon(n)}{1 + \sigma(n)\delta t / \varepsilon(n)}\right\} E(n, m-1) - \frac{\left[H(n+1, m) - H(n-1, m)\right]}{\beta \varepsilon(n)\left[1 + \sigma(n)\delta t / \varepsilon(n)\right]} , \qquad (24)$$

which can be shown to lead to the correct perfect conductivity limit upon time stepping.

The corresponding magnetic field relation is less problematic and results in

$$B(n,m+1) = B(n,m-1) - \frac{1}{\beta}\left(E(n+1,m) - E(n-1,m)\right) . \qquad (25)$$

## 5.0. The Numerical Algorithm

For convenience the algorithm will only contain normalized field components, which we shall denote as e(n, m) and b(n, m). Clearly (24)-(25) are applicable to all layers except the first and last (for they invoke a nonexistent neighboring layer). It is therefore adequate to employ (24)-(25) for $n \in (2, N+5)$, this results in:

$$e(n,m+1) = \left\{\frac{1 - \frac{\sigma(n)\delta t}{\varepsilon_0 \varepsilon_r(n)}}{1 + \frac{\sigma(n)\delta t}{\varepsilon_0 \varepsilon_r(n)}}\right\} e(n,m-1) - \frac{c_0}{\beta}\frac{\left[h(n+1,m) - h(n-1,m)\right]}{\varepsilon_r(n)\left[1 + \frac{\sigma(n)\delta t}{\varepsilon_0 \varepsilon_r(n)}\right]} , \qquad (26)$$

$$b(n,m+1) = b(n,m-1) - \frac{c_0}{\beta}\left(e(n+1,m) - e(n-1,m)\right) . \qquad (27)$$

The above equations must be supplemented by the calculation of the normalized h, from knowledge of normalized b. As we are dealing with materials with no memory as depicted in Figure 3, and described in the text preceding it, the inverse of (11) can be obtained analytically in a few cases, such as the one we use in this presentation. This is not a requirement for the time stepping procedure, as the scheme can accept any nonlinearity, but is however convenient at this early stage. The pertaining space-time local inverse relation h(b) is:

$$h = \left[1 + \left(\frac{1}{mu} - 1\right) e^{-\left[\frac{|b|}{bco}\right]^{\nu}}\right] b . \qquad (28)$$

The fields in the first spatial element can be obtained from (17)-(19) :

$$e(1,m+1) = e(2,m) + \frac{\nu}{2}\left(e(3,m) - e(1,m)\right) + \Psi(m) \qquad (29)$$

$$\Psi(m) = e^{inc}(1,m+1) - e^{inc}(2,m-1) - e^{inc}(1,m) + e^{inc}(2,m) \qquad (30)$$

$$b(1,m) = 2\,e^{inc}(1,m) - e(1,m) \qquad (31)$$

$$h(1,m) = b(1,m) . \qquad (32)$$

Finally, the fields in the last spatial element can be obtained from (20)-(22):

$$e(N+6,m+1) = e(N+5,m) - \frac{\nu}{2}\left(e(N+6,m) - e(N+4,m)\right) . \qquad (33)$$

$$b(N+6,m) = e(N+6,m) \qquad (34)$$

$$h(N+6,m) = b(N+6,m) . \qquad (35)$$

Equations (26)-(35) form the basis of the time stepping scheme. They have been implemented numerically in a series of computer codes, each having a different property, such as optimization of memory allocation, etc.

### 5.1. Implementation

The above equations have been implemented numerically in a FORTRAN code. The resulting Finite Difference Time Domain code is fast and accurate. The most recent version of the code has been optimized to minimize memory allocation, which is done by storing only four historical data sets, and performing cyclic permutation of the data. This has allowed us to perform accurate calculations with a number of time steps in excess of 6 million, a number which is necessary in order to reach a periodic state (sinusoidal input) in the case of highly conducting materials.

The code has been subjected to limited testing involving multiple layer modeling of a linear homogeneous lossy and lossless slab obtained by canonical solution. Specially noteworthy is the check on the correct highly conducting (copper) and perfectly conducting behavior. The agreement with canonical transmission/reflection is excellent, resulting for instance in a .6 dB discrepancy on transmission through a thick Cu slab, for a transmission coefficient of nearly -100 dB (the FDTD model was composed of several layers, typically 10 layers).

With the availability of this code, the door is open for exploration of shielding properties on a number of interesting nonlinear layered magnetic structures.

### 5.2. A New Nonlinear Shielding Effect

The code has been subject to some investigation, in particular, we have done some preliminary study on the effect of profiles (i.e., inhomogeneities) of nonlinear parameters on otherwise homogeneous conductivity and permittivity layers.

The calculations to be presented here will be compared with the characteristic transmission through a layered slab (10 layers) of alternating purely conducting and purely magnetic (isotropic) layers. This structure is shown in Figure 4.

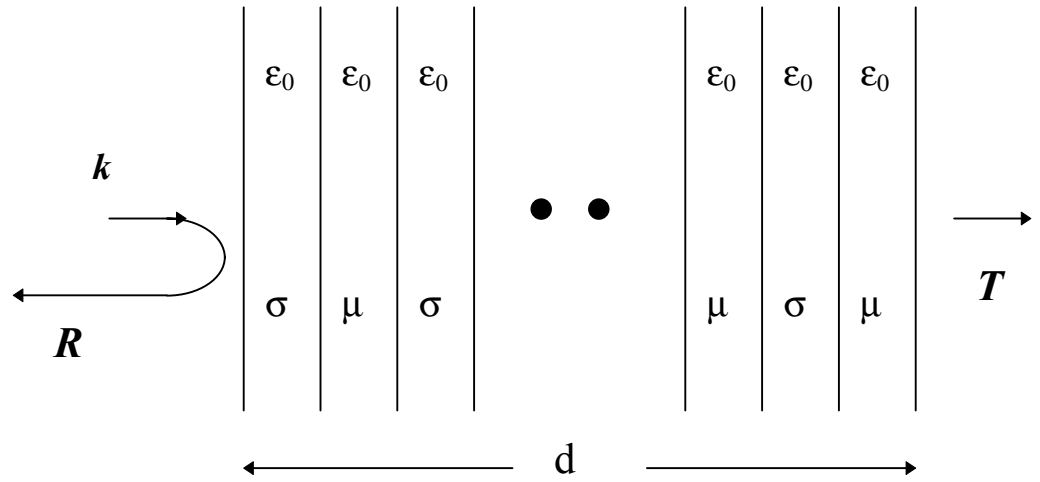


Figure 4. Reference configuration. Ten layers linear alternating structure with free space permittivity, $\sigma = 11.6 \times 10^4$ (i.e., $\sigma_{Cu}$ /500), and $\mu$ (relative) = 2000. The total thickness "d" is 1 micron. The main frequency of interest in this example has been chosen to be 1 GHz, frequency at which the total thickness is of the order of half the effective skin depth.

The response of the reference structure can be approximated by a homogeneous slab of identical thickness, but of average conductivity ($< \sigma > = 5.8 \times 10^4$) and average permeability ($<\mu > = 1000$). For convenience, the exact solution to this approximate problem has been calculated and included as Figures 5 and 6 which correspond to thickness (in skin depth units) and magnitude of transmission coefficient, both on the frequency range .5 GHz to 2 GHz. The figures indicate that we are dealing with a wide-bandwidth structure.

The exact response to the geometry of Figure 4 has been calculated via our newly developed FDTD code. The data is presented in Figure 7 for a frequency of 1 GHz, and a number of three million time steps, with a model consisting of one numerical layer representing each physical layer. The data has been sampled every 5000 time steps, and has been allowed to reach what we consider to be "steady state". Previous runs indicate that by the second peak of a sinusoidal response we are typically in the periodic response regime, away from the range of influence of the transient response. The agreement between Figure 6 and Figure 7 is good as expected since we are dealing with only 10 layers, 5 pairs, for which an effective medium is a crude estimate[1].

[1] This example is not a test for our FDTD code (which has successfully undergone testing using an exact model).

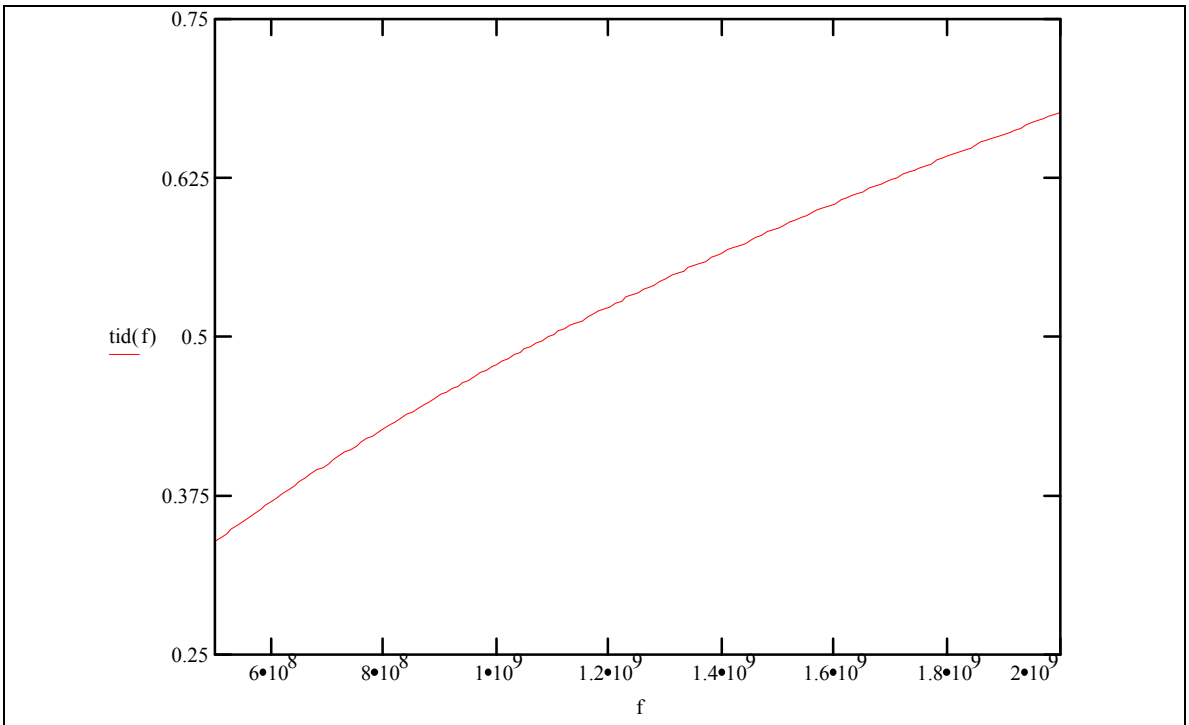


Figure 5. Thickness of approximate (homogeneous) reference structure in skin depth units.

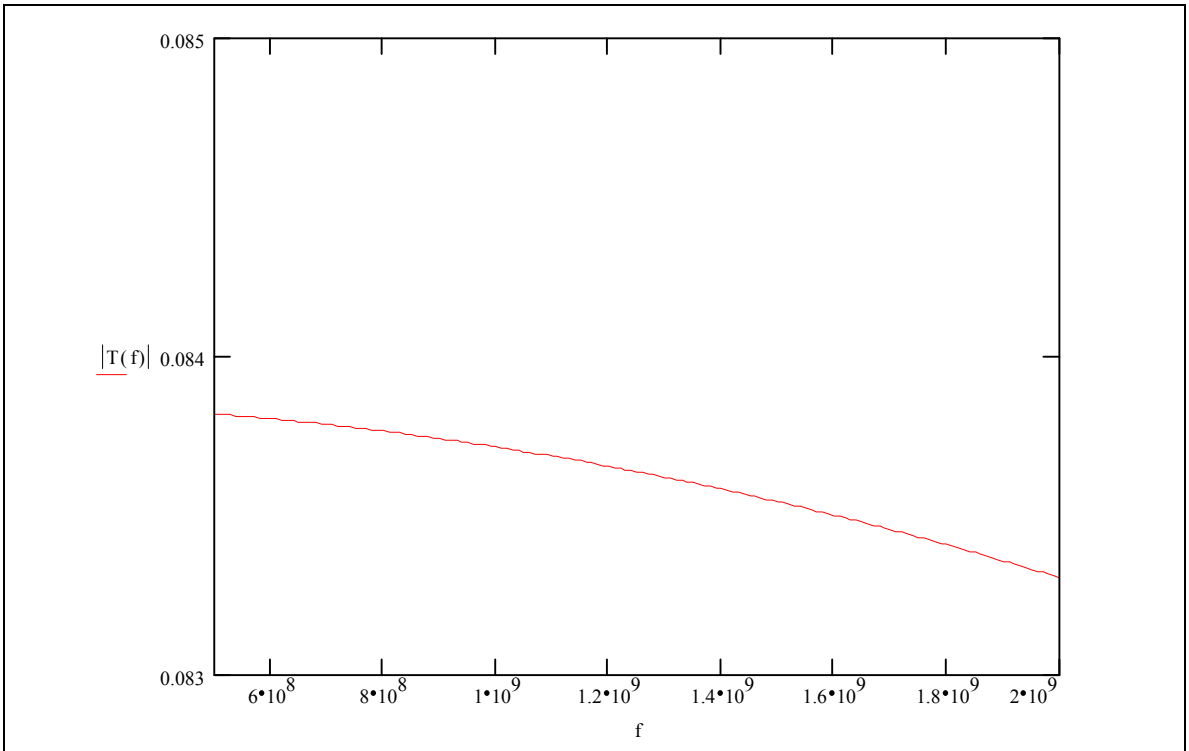


Figure 6. Magnitude of transmission coefficient of approximate (homogeneous) reference structure.

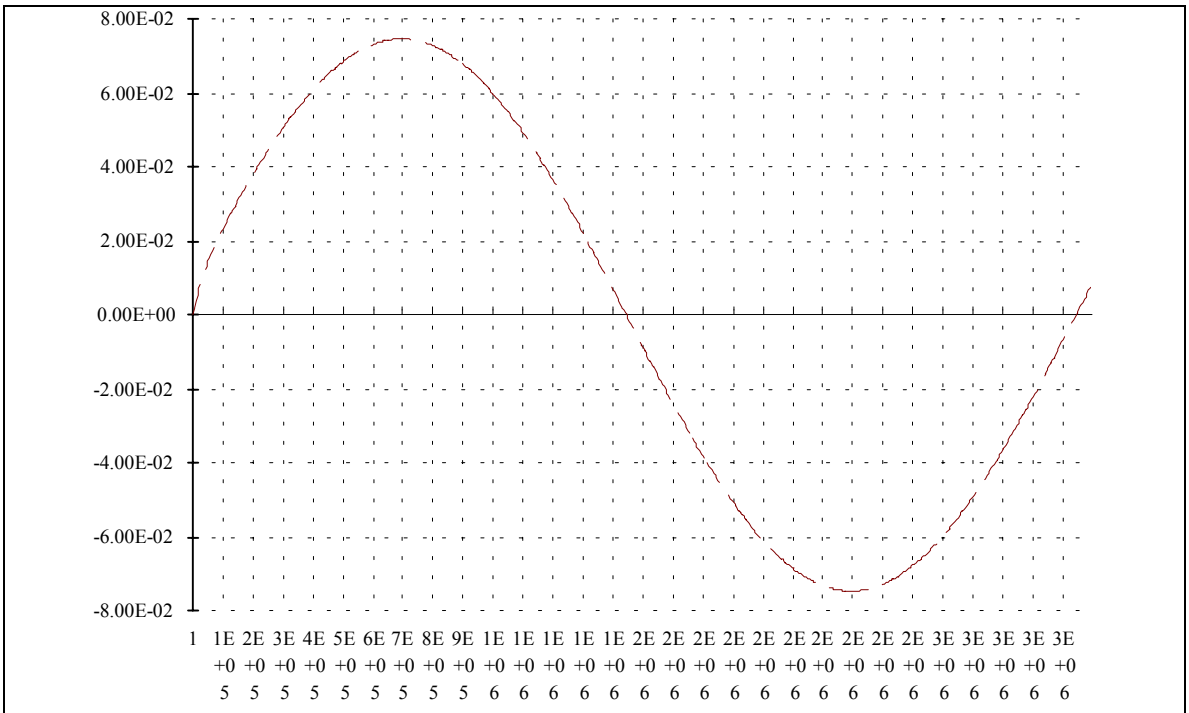


Figure 7. FDTD solution to the reference geometry of Figure 4 at 1 GHz. The graph shows the transmission as a function of time(measure in time steps, for a total of 3 million).

### 5.3. Effect of profile in nonlinear parameters

In the course of this investigation we have dealt with several profiles. The one we present here is one which shows what appears to be the basic character of a novel solution. The model consists of 10 layers of homogeneous $\sigma$ (=< $\sigma$ > above) = $5.8 \times 10^4$ and mu (=<$\mu$ >) = 1000, which was introduced in the model (28). In addition, bco has the profile shown in Table II, and is essentially a straight line going from a maximum of 1000 on the illuminated side, to a minimum of 100 on the transmitted side.

The FDTD solution is presented in Figure 8. It can be observed that the transmitted field is in the form of a sinusoid after passing through a limiter. The peak value being roughly $.3\times10^{-2}$, i.e., ≈ 8 dB below the transmission coefficient of the reference geometry. At this point we can only speculate as to the formation of the signal. It appears that the distributed nonlinearity interacts with the locally delayed and attenuated signal in a manner that reinforcement can occur. A local switching in magnetic properties does not only change the propagating medium, but also generates electric and magnetic fields which can be made to interact destructively with the traveling signal in the forward direction, and which can be tailored to escape out of the saturated medium in the backward direction (producing extra insertion loss). If this simplified picture is correct, it may be possible to design a profile of nonlinear parameters such as to achieve "synchronism", thereby reducing the transmitted field to a minimum.

Table II

| N (layer No) | bco(n) |
|---|---|
| 1 | 1000 |
| 2 | 900 |
| 3 | 800 |
| 4 | 700 |
| 5 | 600 |
| 6 | 500 |
| 7 | 400 |
| 8 | 300 |
| 9 | 200 |
| 10 | 100 |

We have achieved roughly 8 dB without optimization. We speculate the improvement in shielding properties can be made significantly more substantial. Consider for instance the bandwidth on transmission. We have done calculations on the above linear profile for .5 GHz (with 6 million time steps) and 2 GHz (with 3 million time steps), and the resulting transmission data is presented in Figures 9 and 10 respectively. The figures show that the effect has a large bandwidth, with no significant difference on transmission over this 4:1 frequency range, which at this point might not be surprising in view of the frequency response of the approximate (homogeneous) reference structure whose transmission was shown in Figure 6. In addition, from experience with circuit theory, nonlinear and eminently non-dispersive switching networks (such as banks of fast diodes) have large bandwidths. Because of this simulation we believe we will not only be able to improve the shielding at a given frequency, but possibly over a wide bandwidth.

To give further confidence in the proposed scheme, we present another calculation. This time we have a semi-exponential profile for bco. The profile is presented in Table III, and roughly corresponds to an exponent of .8, which essentially connects the extreme values of the previous linear profile. The transmitted signal, for an incident field of frequency of 1 GHz, has been calculated with 3 million time steps and is shown in Figure 11. The transmission peak is now $2.5\times10^{-2}$, i.e., $\approx$ 9.5 dB below the transmission coefficient of the reference geometry. This indicates that a slight reshaping of the linear profile has resulted in an additional 1.5 dB gain in insertion loss.

Table III

| n (layer No.) | bco(n) |
|---|---|
| 1 | 1000 |
| 2 | 800 |
| 3 | 640 |
| 4 | 500 |
| 5 | 400 |
| 6 | 320 |
| 7 | 250 |
| 8 | 200 |
| 9 | 160 |
| 10 | 130 |

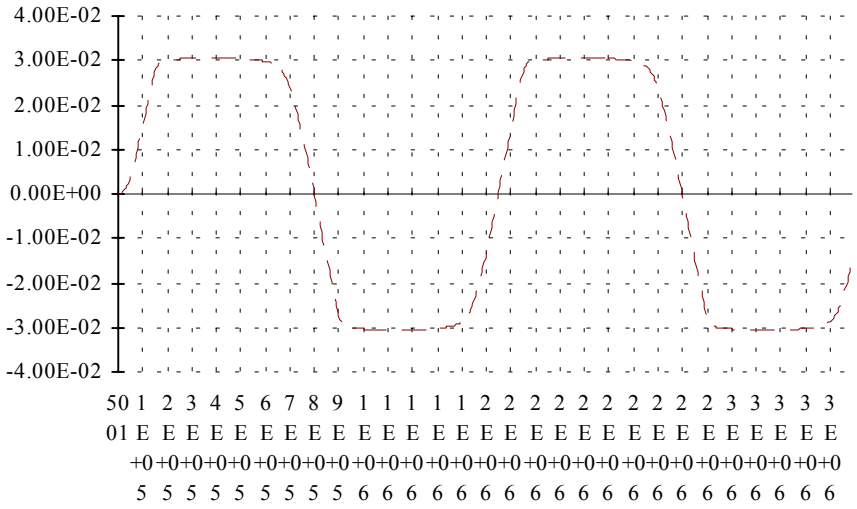


Figure 10. FDTD solution to the 10 layer nonlinear structure specified by the parameters of Table II at 2 GHz.

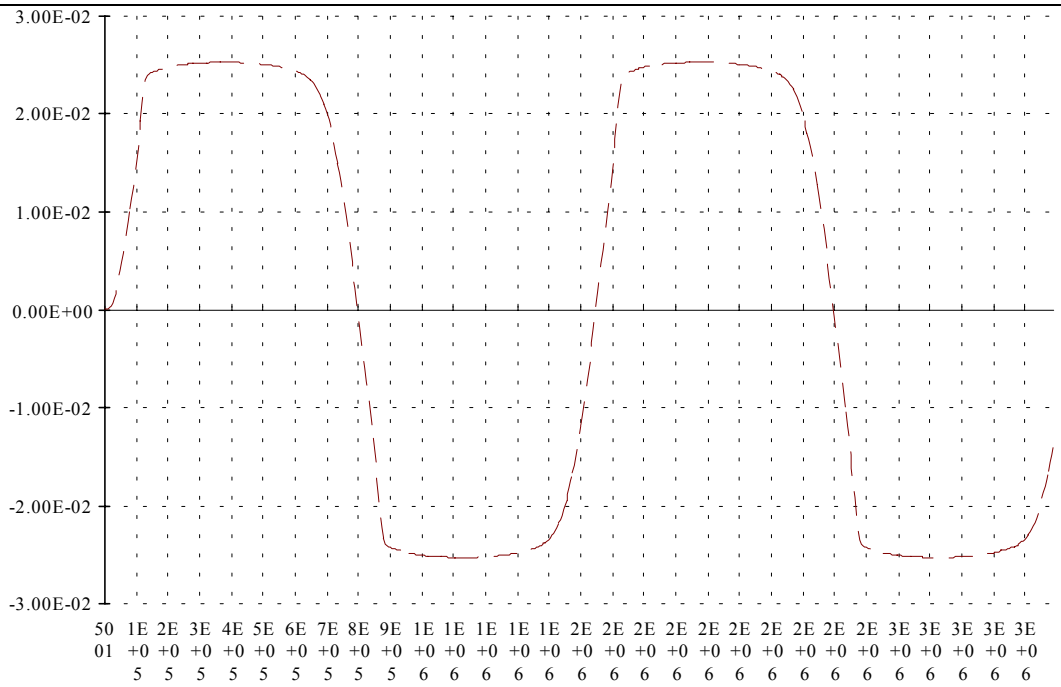


Figure 11. FDTD solution to the 10 layer nonlinear structure specified by the parameters of Table III at 1 GHz.

## 6.0. Material Fabrication

The fabrication method and total cost for making the multilayer system will have a strong influence on the marketing of the product. EM shielding is a highly fragmented market, which severely limits the capital cost of any new processes as well as the production cost of any new shielding material.

Except for space applications, added weight rarely has a high cost penalty and a light material with very good SE must meet these cost constraints. The proposed system has the potential of filling a niche market, that works with high fields which would saturate most materials. The limited size of this market also limits the investment potential, which limits the capital cost available to setup a fabrication system.

To be competitive, the startup cost of the capital equipment needed to manufacture the film has a strong influence on the decision to commercialize the material. In mature technologies or those with a proven record, the cost of the money associated with the capital equipment cost is factored into the cost to produce the material. For an unproved technology and undefined markets, it is important to minimize the amount of money at risk and a low startup cost for a manufacturing is desirable. The cost of materials is also an important consideration since this strongly affects the final cost.

### 6.1. Material Selection

The structure consists of alternating layers of a film with a high $\sigma$ and a high $\mu$. For the high $\sigma$, copper is the film of choice. It has high conductivity and is low cost. It can be deposited easily using sputtering, electron beam deposition or electro-less or electro-plating.

The easiest magnetic film to deposit is one of the Ni/Fe alloys (permalloy). Permalloy is a soft magnetic film. It is magnetostrictive with zero magnetostriction occurring at about the 81/19% Ni/Fe ratio while the higher Fe compositions have higher saturation fields. As a thin film, it exhibits a uniaxial anisotropy with both an easy and hard axis in the plane of the film. This anisotropy is controlled by a wide variety of factors including the angle of incidence of the depositing atoms, the internal stress in the film and can be introduced by biasing the film during growth with a magnetic field.

### 6.2. Electrodeposition

Electrodeposition is the standard production process for depositing thicker layers of copper. The lower capital cost and the ability to deposit thick layers makes it the process of choice for thick films. It is low cost with electrodeposited copper foil 10-20 micron thick only slightly more expensive than the cost of bulk copper. Since the total film thickness of the final coating is desired to be 20-50 microns, this is attractive.

Copper can be deposited by either electro-less or electrolytic deposition. The electro-less deposition can be used to deposit the starting conductive coating onto an insulating substrate (for example, a composite structure).

Plating of an alloy is more complex than a single component system. The plating potential of iron and nickel are not the same and adjustments in the final concentration are obtained by changes in the relative concentration of the Fe/Ni ion and changes in the bath composition. Many are based on two early baths; one patented in 1931 by Burns and Warner[7] and a second by Wolf and McConnel. They start with the Watts Bath for plating nickel and add iron to form the alloy. For the plating in the Phase I program, a joint program was initiated with a local industrial plater (Advanced Plating Inc.). They had experience with magnetic electrodeposition along with required permits for waste generation. A commercial bath for Ni/Fe is available (Niron) which is marketed as a low cost alternative to plating Ni where corrosion protection is desired. The Phase I program had planned to use this commerical bath but it is currently not available in smaller quantities.

A number of films were deposited , using the following recipe. with the bath operated at $50^0$C. This is basically the original bath, developed by Burns and Warner, with the bath operated at $50^0$C. This is designed to produce a 80/20 nickel/iron permalloy film, which is the zero magnetostriction film. This bath had considerable with stress in the film. The Niron bath included stabilizers and brighteners, which helped to control adhesion. Films were plated with this bath but in general, there magnetic properties were poor and this was attributed to the high stress, which affected the magnetic properties.

| | |
|---|---|
| $NiSO_4*6H_2O$ | 212.0 g/l |
| $FeSO_4*7H_2O$ | 22.0 g/l |
| $NiCl_x*6H_2O$ | 18.0 g/l |
| $FeCl_x*4H_2O$ | 2.5 g/l |
| $H_2BO_3$ | 25.0 g/l |
| $Na_2SO_4*10H_2O$ | 180.0 g/l |

Measurements on these films were limited to the magnetic properties only. With better films, due to the high shielding performance, conventional techniques such as TEM cells are not suitable for this use. One technique is the use of Helmholtz coils with the film fabricated as a cylinder, a technique similar to IEEE standard 299-191 [8] and discussed in [5]. A loop antenna is placed in the center of the cylinder and a large set of Helmholtz coils is used to generate the magnetic field. This approach has the advantage that the performance can be predicted and compared with experiment. In addition, magnetic and electrical shielding can both be resolved on the single measurements, as shown in Figure 12 (from [5]). This is the technique planned for the routine testing of the multi-layer films.

A second advantage of this approach is that, since the sample size is relatively small, high fields are easier to generate. This approach will thus allow us to experimentally verify the calculations on the behavior at higher fields.

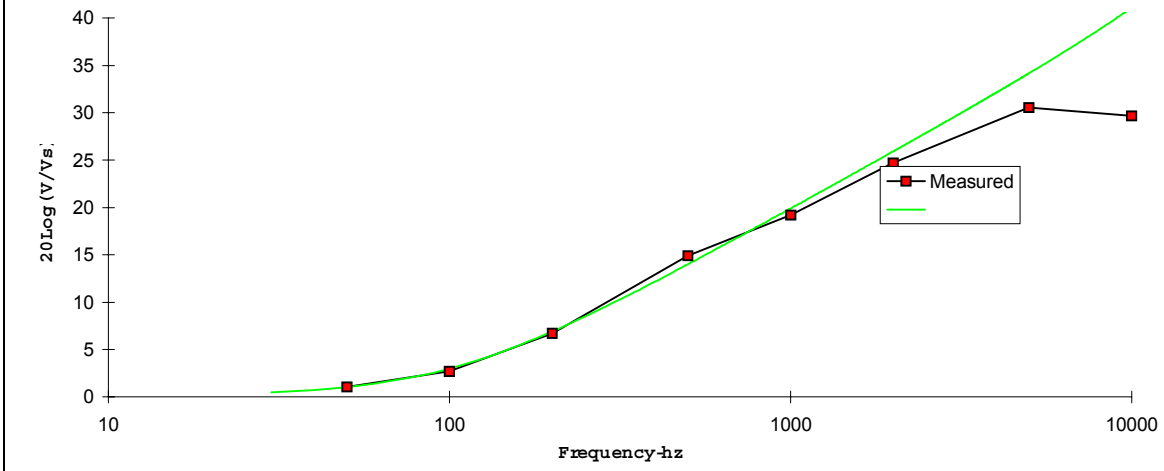


Figure 12. Measured and calculated shielding for cylindrical shapes. Calculations based on Schelkunoff[9]. Results from ref. [5].

**References**

[1] Handbook on EM Control Methods and Techniques, Dan White Ed., Dan White Consultants.
[2] L.E. McBride and Y.Trenkler, Proceedings of the IEEE National Symposium on EMC, 1084, pp. 261-263.
[3] L.E. McBride and Y. Trenkler, Proceedings of the IEEE National Symposium on EMC, 1990.
[4] W.J. Biter, P.J. Jamnicky and W.Coburn, ITEM. R&B Enterprises, p.128, February, 1995.
[5] W.J. Biter, P.J. Jamnicky and W.Coburn, 7th International SAMPE Conference, Parsippany, NJ, p. 234, 1994.
[6] W. Coburn et al, Journal of Radiation Effects, Vol. 31, No. 1, Jan. 1995.
[7] Patient 3,691,031.
[8] Institute of Electrical and Electronic Engineers, pp. 299-191.
[9] S.A. Schelkunoff, Bell System Technical Journal 13, 1934.

# 7.0. Recommendations

## 7.1. Proposed Analytical Work

Nonlinearity in magnetic shielding problems is usually seen as an undesirable effect, this is in view of the fact that when a magnetic material is saturated its magnetic properties (as measured via an effective permeability) vanish. What is not appreciated is that nonlinearity produces switching, thereby causing decomposition of the original signal into time harmonic components leading to inherent energy loss at the frequency of interest (the frequency multiplication relying on the steepness of the B-H curve). What is more important, is that the simplified concept arising out of DC (saturation) magnetic conditions may not be fully representative of all possible nonlinear solutions to the field equations. Take for instance the case of the novel nonlinear optical fibers wherein the nonlinearity results in solution like solutions with impressive reduction in dispersion and effective losses.

Such a behavior could not have been hypothesized out of the simplified picture of a fully polarized dielectric rod.

Based on preliminary but sound numerical data, we strongly believe that the advantages of nonlinearity in magnetic shielding situations have not been fully explored. The purpose of this work is to utilize the nonlinearity of the magnetic layers to demonstrate the feasibility of a new wide bandwidth shielding material.

For the Phase II program, we propose to establish the theoretical foundation of the new composite, and to ascertain that the new material can be produced having the desired shielding capacity while being lightweight, flexible, and cost effective.

The proposed analytical effort should address the following items:

- **Elucidate the reason for the increased shielding.** This analytical and numerical effort will have as its objective the isolation and exploitation of the physical phenomena responsible for the increased shielding effect.

- **Attempt to analytically harness the new principle.** If successful this item will result in the determination of canonical nonlinear solutions.

- **Numerical optimization to define optimum profiles**. Substantial effort will be invested in the search of nonlinear solutions which enhance the shielding properties of the new material.

- **Enhancement in code testing.** The plan is to design a robust computational tool which incorporates a detailed numerical model, and to achieve this we need to perform extensive validation, including the generation of (check case) canonical solutions.

- **Code development, new capabilities.** This will include enhanced accuracy, inclusion of a diverse family of nonlinear curves, some of which will require a special routine devoted to the solution of the inverse H(B) problem.

- **Inclusion of a user interface to make it friendly and commercially attractive**. We expect the code to be able to be commercialized as a stand alone product. We also expect to integrate the code with a graphics package for quick production of time domain "snapshots", and harmonic analysis.

## 7.2. Shielding Material

The proposed layered structure will have superior electromagnetic shielding properties at a lower cost and lighter weight. Due to the projected high field behavior, it will be of special interest for the military, especially in applications such as the rail gun and others requiring high SE in high fields. Conventional applications will include shielding from hazardous electromagnetic radiation (homes, schools), sensitive equipment shielding, and medical applications.

The production of the multilayer films is separate from the experimental code verification. The plating of the small 1-2 ft. wide strips are necessary to verify the code. This will also be a necessary part of marketing the code. The processes from the Phase I will be sufficient to plate film large enough for this verification. Larger sizes and lower cost necessary for production require additional capital. This will be obtained during the Phase II program with the profits from the sale of the code.